Levitation and Movement of Tripalmitin-Based Cationic Lipospheres on a Dielectrophoresis-Based Lab-on-a-Chip Device

Enrica Fabbri,[1] Monica Borgatti,[1,2] Nicolò Manaresi,[3] Gianni Medoro,[3] Claudio Nastruzzi,[4] Silvia Di Croce,[4] Azzurra Tosi,[4] Stefania Mazzitelli,[4] Irene Mancini,[1] Roberto Guerrieri,[5] Roberto Gambari[1,2]

[1]*Laboratory for the Development of Pharmacological and Pharmacogenomic Therapy of Thalassemia, Biotechnology Center, University of Ferrara, Ferrara, Italy*
[2]*ER-GenTech, Department of Biochemistry and Molecular Biology, University of Ferrara, Ferrara, Italy*
[3]*Silicon Biosystems, Bologna, Italy*
[4]*Department of Medicinal Chemistry and Pharmaceutics, University of Perugia, Perugia, Italy*
[5]*Center of Excellence on Electronic Systems, University of Bologna, Bologna, Italy*

Received 27 June 2007; accepted 10 January 2008
DOI 10.1002/app.28413
Published online 2 June 2008 in Wiley InterScience (www.interscience.wiley.com).

ABSTRACT: Dielectrophoresis (DEP) is a very valuable approach for designing and developing laboratory-on-a-chip (lab-on-a-chip) devices that are able to manipulate microparticles and cells. Lab-on-a-chip technology will enable laboratory testing to move from laboratories using complex equipment to nonlaboratory settings. We used a lab-on-a-chip device, the SmartSlide, which carries 193 parallel electrodes and generates up to 50 cylinder-shaped DEP cages able to entrap microparticles and cells within DEP cages and move them along the chip. For lab-on-a-chip technology, the characterization of microparticles exhibiting a differential ability to be DEP-caged, levitated, and moved is important for the development of both diagnostic and therapeutic protocols. We determined whether the SmartSlide could be used to levitate and move tripalmitin-based lipospheres carrying increasing concentrations of dihexadecyl dimethyl ammonium bromide (DHDAB) as a cationic surfactant. The data obtained with this DEP-based platform showed that DEP caging, levitation, and movement of the cationic lipospheres depended on the percentage of DHDAB. Tripalmitin lipospheres containing 6% DHDAB could be DEP-caged and manipulated. On the contrary, lipospheres containing 12% DHDAB did not exhibit an efficient ability to be DEP-caged and moved throughout the chip. To our knowledge, this is the first report on the possible use of a DEP-based lab-on-a-chip device for guided manipulation of lipospheres. This information might be of interest in the fields of drug discovery, delivery, and diagnosis. © 2008 Wiley Periodicals, Inc. J Appl Polym Sci 109: 3484–3491, 2008

Key words: bioengineering; biopolymers; drug delivery systems

INTRODUCTION

We have demonstrated that dielectrophoresis (DEP)-based laboratory-on-a-chip (lab-on-a-chip) devices are suitable for (1) programmed levitation and movement of eukaryotic cells[1–4] and (2) programmed delivery of microspheres to target cells.[5,6] This is in line with the concept that lab-on-a-chip technology will enable laboratory testing to move from laboratory using complex equipment to nonlaboratory settings.[7,8] As is well known, DEP[9–13] has been reported as a very valuable approach in projects aimed to design and produce lab-on-a-chip devices able to manipulate microparticles and cells.[14–18]

The application of DEP protocols results in the movement of particles in nonuniform electric fields.[1,3] If the field is nonuniform, the particles experience a translational force (DEP force) of magnitude and polarity, depending not only on the electrical properties of the particles and medium but also on the magnitude and frequency of the applied electric field. This means that for a given particle

Correspondence to: R. Gambari, Department of Biochemistry and Molecular Biology, University of Ferrara, Via Fossato di Mortara 74, 44100 Ferrara, Italy (gam@unife.it).

Contract grant sponsor: Ministero dell' Università e della Ricerca (MIUR)-COFIN-2000 and European Union (EU) MEDICS Project; contract grant number: IST-2001-32437 (to R. Guerrieri).
Contract grant sponsor: MIUR-COFIN-2002 (''Applications of a Dielectrophoresis-Based Lab-on-a-Chip to Diagnosis and Drug Research and Development;'' to R. Gambari).
Contract grant sponsor: Fondo per gli Investimenti per la Ricerca di Base-2001 (''Development of a Lab-on-a-Chip Based on Microelectronic Technologies and Its Biotechnological Validation;'' to R. Guerrieri, R. Gambari, and C. Nastruzzi).
Contract grant sponsor: Fondazione Cassa di Risparmio di Padova e Rovigo.
Contract grant sponsor: Fondazione Italiana Ricerca sulla Fibrosi Cistica.
Contract grant sponsor: Association Italiana per la Ricerca sul Cancro.
Contract grant sponsor: Associazione Veneta per la Lotta alla Talassemia (AVLT, Rovigo, Italy).

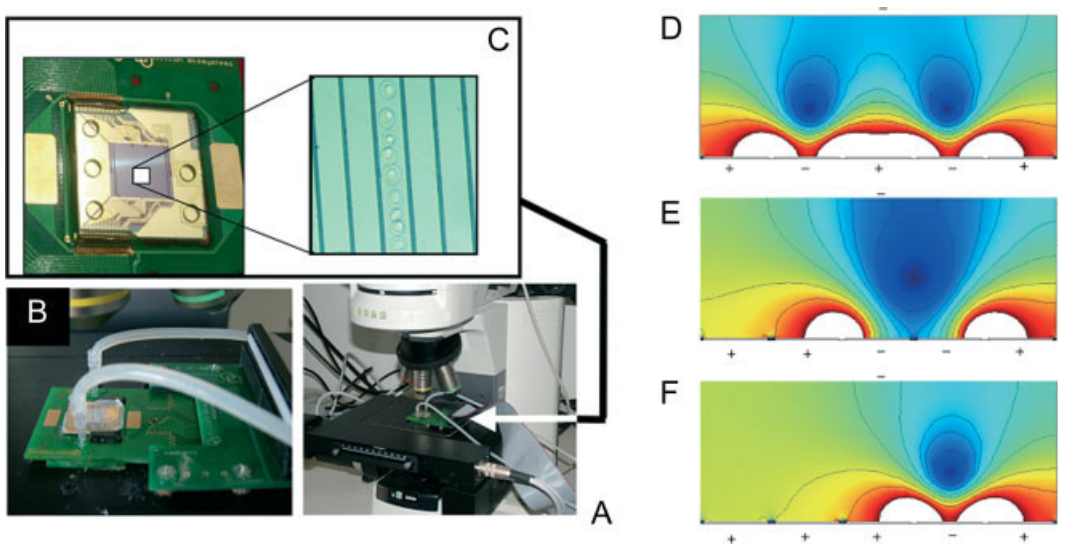

Figure 1 Setup of the lab-on-a-chip assembly. (A) The lab-on-a-chip device is located under a microscope and in connection with the motherboard. (B) The location of the DEP device is shown. (C) The structure of the SmartSlide is shown; in the insert, the entrapment of K562 cells within a cylinder-shaped DEP cage is shown. (D) Two DEP cages are forced to move against one another, leading to (E) a single cage, which (F) can be further moved. [Color figure can be viewed in the online issue, which is available at www.interscience.wiley.com.]

type and suspending medium, the particle can experience, at a certain frequency of the electrode applied voltages, a translational force directed toward regions of high electric field strength (this phenomenon is called *positive DEP*). Alternatively, by a simple change in the frequency, it may experience a force that will direct it away from regions of high electric field strength (this phenomenon is called *negative DEP*).[1,3]

The application of DEP-based devices for software-guided manipulation of microspheres in drug delivery and immunophenotyping of target cells has been recently reported.[1,5]

In addition to liposomes and microspheres, lipospheres (LSs) can be very useful in experiments aimed at the delivery of drugs to target cells and tissues.[19–24] LSs represent a particular type of nonviral vectors constituted of a mixture of neutral lipids (generally triglycerides) and, when required, positively charged lipids that can interact with negatively charged nucleic acid molecules [cationic lipospheres (CLSs)]. CLSs are solid microparticles with a mean diameter usually between 0.2 and 500 μm,[25] CLSs present several advantages, including a high drug loading capacity, good physical stability, low cost of ingredients, and ease of preparation. Moreover, lipidic LSs combine the advantages of polymeric particles, fat emulsion, and liposomes, and avoid some of the disadvantages typical of liposomes.[25] For these reasons, lipid-based microparticles have been successfully proposed for the delivery of a variety of conventional drugs, including antibiotics,[26] anti-inflammatory compounds,[27] vaccines and adjuvants.[28]

In this study, we characterized tripalmitin (TP)-based LSs carrying different concentrations of dihexadecyl dimethyl ammonium bromide (DHDAB or $DDAB_{16}$) as a cationic surfactant, with respect to (1) antiproliferative effects, (2) binding to DNA, and (3) DEP properties with the SmartSlide lab-on-a-chip device (Silicon Biosystems, Bologna, Italy).

EXPERIMENTAL

Hardware and software

Figure 1 shows the equipment we used, which included a Nikon Eclipse 80i microscope (Nikon Instruments, Sesto Fiorentino, Italy) [Fig. 1(A)], a motherboard, a platform for allocation of the DEP-based device [Fig. 1(B)], a computer, and the SmartSlide [Fig. 1(C)],[1] for the manipulation of microparticles after the generation of cylinder-shaped DEP cages. The levitation, movement, and separation of cells and particles could be monitored in real time.[1,3] The SmartSlide [Fig. 1(C)] was composed of a microchamber, delimited on the top by a conductive and transparent lid (which was itself an electrode and was electrically connected to the SmartSlide by means of a conductive glue) and on the bottom by a support. A spacer (composed of optic fibers) determined the chamber height, whereas a silicon elastomer gasket delimited and sealed the microchamber on the sides. This device had 193 parallel electrodes by which it was

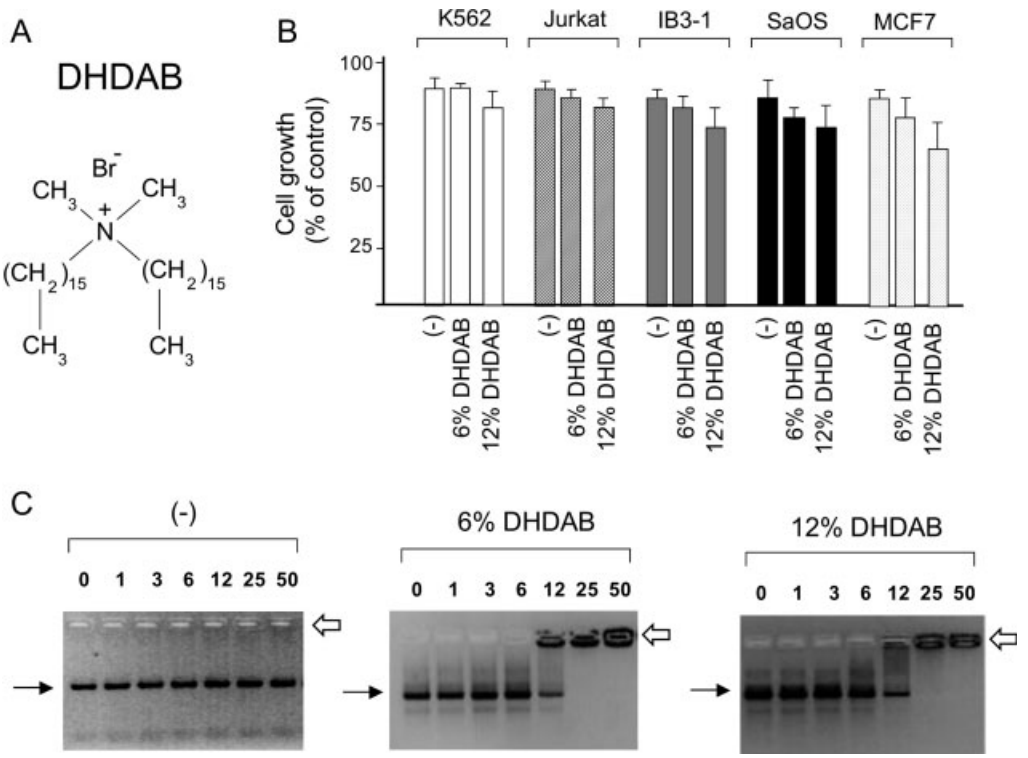

Figure 2 (A) Chemical structure of DHDAB. (B) Effects of neutral LS(−), 6% DHDAB–CLS, and 12% DHDAB–CLS on cell proliferation (assayed after 4 days of cell culture) of human K562, Jurkat, IB3-1, SaOS-2, and MCF7 cells. The results (cell number/mL) are expressed as the percentage of control untreated cells plus or minus the standard deviation (three independent experiments). (C) DNA binding of neutral LS(−), 6% DHDAB–CLS, and 12% DHDAB–CLS. Complexation with DNA is shown by the shift in the upper part of the gels (open arrows). The solid arrow shows a free DNA probe.

possible to generate 0 to 50 cylinder-shaped DEP cages. The motherboard was used to generate and distribute to each electrode in the device the proper phases needed to create and move the DEP cages and to perform the sensing operations, whereas a software tool allowed us to control the actuation and sensing operations flows. By changes in the electrode programming, each DEP cage could be independently moved from electrode to electrode along the whole microchamber, dragging with it the trapped elements. This device allowed the separation and/or concentration of cells and microspheres in a fully electronic system without the need for fluid flow control, which tends to be bulky and expensive in an integrated system perspective. The design, technical parameters, building approach, and manufacturing of this DEP-based device were described by Medoro et al.[1]

Cultured tumor cell lines

The cells used in this study were from the human K562 leukemia cell line, which was developed by Lozzio and Lozzio[29] from a patient with chronic myelogenous leukemia in blast crisis and has been used by our group in several research projects.[30,31] This cell line exhibits good interactions with cationic liposomes and microspheres.[32] Cells were cultured in Roswell Park Memorial Institute medium, 10% FCS, at 37°C in 5% CO_2. Before manipulation within the SmartSlide, the K562 cells were washed and resuspended in 280 m*M* mannitol and 6.25 m*M* KCl. Other cell lines that have been used to test possible antiproliferative effects of LSs include the human T-lymphoid Jurkat,[33] tracheal epithelium IB3-1,[34] osteosarcoma SaOS-2,[35] and breast cancer MCF7.[36]

Production of the LSs

TP and DHDAB were obtained from Fluka Chemical Co. (Buchs, Switzerland). Glyceryl monostearate was from Gattefossè (Saint-Priest Cedex, France). Poly(vinyl alcohol) (PVA; Airvol 205) was from Air Products Corp. (Allentown, PA). An amount of 0.5 g of TP and the required DHDAB were melted at 70–75°C and then emulsified into 15 mL of an external aqueous phase containing PVA as the dispersing agent. The employed LSs were constituted by TP and stearic acid in a 4 : 1 ratio and by DHDAB. The chemical structure of this cationic molecule is shown in Figure 2(A). The produced LSs were isolated by filtration. Microparticle morphology, size, and size distributions were determined by optical and electron

microscopy observations, as described elsewhere.[25] For the optical analysis, a Diaphot optical microscope (Nikon) was used. For the electronic analysis, microparticles were metalized by gold coating (Edwards sputter coating S150) and analyzed at 15–20 kV by a Stereoscan 360 scanning electron microscope (Cambridge Instruments, Cambridge, United Kingdom). Microparticle recovery efficiencies were calculated as the percentage of weight of the obtained microparticles, with the total amount of polymer used for the preparation taken as a reference.[34]

Analysis of the electrophoretic mobility of the CLS–DNA complexes

The differential ability of CLSs to bind DNA molecules was determined by electrophoretic mobility shift assay performed on a 2% agarose gel with Tris-Acetate EDTA (TAE) as a running buffer. The target DNA was prepared by the polymerase chain reaction (PCR) with 100 ng of genomic DNA as the template and primers amplifying a portion of the β-actin gene. The forward primer was 5′-TGA CGG GGT CAC CCA CAC TGT GCC CAT CTA-3′; the reverse primer was 5′-CTA GAA GCA TTT GCG GTG GAC GAT GGA GGG-3′. Amplifications were performed in 25-μL volumes containing 125 ng of genomic DNA, 0.07–0.3 μ*M* PCR primers, 65 μ*M* deoxyribonucleotides triphosphate (dNTPs), and 1 unit of the DyNAzyme *Taq* polymerase (Finnzyme, Espool, Finland). After an initial denaturation of 6 min at 96°C, a hot start was carried out by the addition of *Taq* polymerase. PCR conditions were as follows: denaturation at 94°C for 1 min, annealing at 63°C for 1 min, an extension at 72°C for 1 min. To study DNA–LS interactions, increasing amounts of LSs were incubated for 10 min in borate buffer (0.28 m*M* $Na_2B_4O_7$ and 10 m*M* H_3BO_3, pH 7.4). DNA molecules were detected by ethidium bromide staining and quantified with a BioRad Gel Doc 2000 (BioRad Laboratories, Milan, Italy).

Cell proliferation assay

The cytotoxicities of different CLS formulations were tested on different human cell lines by a CellTiter 96 cytotoxicity assay kit (Promega Italia, Milano, Italy) according to the indicated instructions. Cells were seeded in a cell culture medium and grown in the presence or absence of increasing amounts (0, 10, 60, 120, 250, and 500 μg/mL) of CLSs. After 72 h, the cell number was determined by a colorimetric procedure.

The developed color was measured at 570 nm (milliOD$_{570}$), and the values obtained, proportional to the number of cells, were plotted as function of the CLS concentration.

RESULTS

DEP-based levitation and movement of biological and physical objects and computer-aided simulation of DEP-forced interactions of the DEP cages

In the insert of Figure 1(C), a representative example is shown to demonstrate the entrapment within a cylinder-shaped DEP cage of several K562 cells. The SmartSlide was able to generate up to 50 DEP cages, which could be moved throughout the lab-on-a-chip device. Figure 1(D,E) shows a numerical simulation of the effects of the general working principle of DEP. By applying suitable potentials to the electrodes, we could generate time-dependent electric fields in the liquid. These fields could then generate DEP fields acting on the particles in the fluid. A DEP force was then generated thanks to the differences in the dielectric permittivities of the different materials. An important point of this approach is that the overall system could be designed to force the DEP fields to create closed cages that could trap inside particles in a stable way [as shown in the insert of Fig. 1(C)]. In Figure 1(D), two cages are simulated, which could entrap, when suitable electric potentials were applied to the electrodes, LSs, microspheres, and/or target cells. By looking at Figure 1(D), one can see a local minimum of electric fields associated with the presence of the two DEP cages. Because these electric potentials could be applied under software control, it was possible to change how particles were moved by the modification of the settings on a computer. In addition, it was possible to change in real time the location of these closed DEP cages. After the potentials applied to electrodes were changed, the location of the two cages changes [Fig. 1(D,E)] and all entrapped LSs were now concentrated within a single DEP cage, which could be moved further [Fig. 1(F)].

Cytotoxicity and DNA-binding activity of CLSs

Figure 2(A) shows the chemical structure of DHDAB. The *in vitro* study performed for the determination of the cytotoxic activity of the two used CLSs demonstrated that low toxicity (in term of antiproliferative effects) on the human leukemic K562 cells was displayed by both 6% DHDAB and 12% DHDAB–LS [Fig. 2(B)]. Neutral LSs were also not toxic under these experimental conditions. K562 cells were cultured for 4 days without LSs or in the presence of 50 μg/mL of neutral LSs or 6 and 12% DHDAB–CLSs. At day 4, the untreated control cells were in the log phase of cell growth. The cell growth was determined by the CellTiter 96 cytotoxicity assay kit according to the measurement of the developed color at 570 nm (milliOD$_{570}$). The values

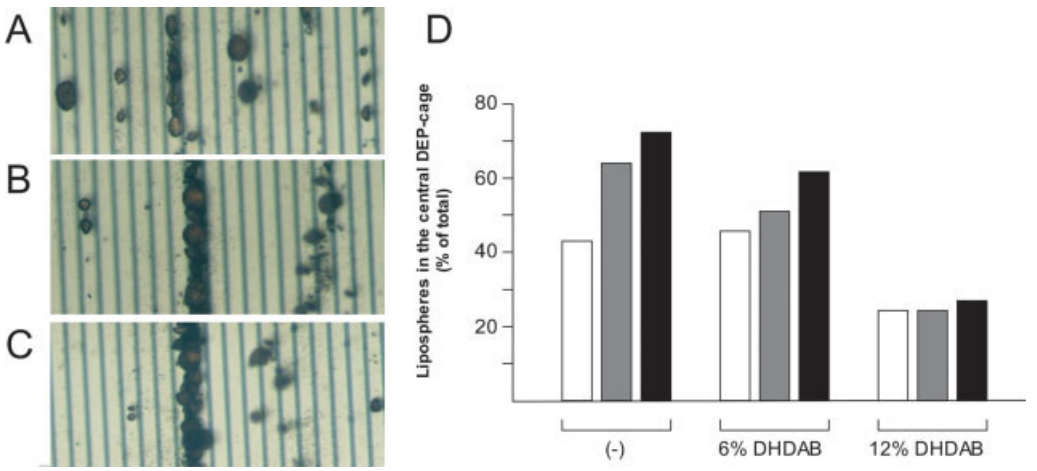

Figure 3 Representative experiment showing the concentration of neutral LS in the central DEP cage after (A) one, (B) two, and (C) three rounds at 100 kHz and 1.6 V. (D) Focusing of neutral LS(−), 6% DHDAB–CLS, and 12% DHDAB–CLS, as indicated after one (open box), two (gray box), and three (black box) rounds of concentration at 100 kHz. Data are expressed as the percentage of LS that were DEP-caged and moved to the SmartSlide central electrode. [Color figure can be viewed in the online issue, which is available at www.interscience.wiley.com.]

obtained by analysis of the neutral LSs and CLSs were compared to those of the control untreated cells.

As shown in Figure 2(B), only slight inhibitions (4 and 12% inhibitions) of K562 cell growth were observed when treatment with 50 μg/mL of 6 and 12% DHDAB–CLS was compared to that of neutral LSs. Similar results have been obtained with other cell lines, including the T-lymphoid Jurkat,[33] tracheal epithelium IB3-1,[34] osteosarcoma SaOS-2,[35] and breast cancer MCF7[36] cell lines. DHDAB–CLS containing a higher concentration of DHDAB (18 and 24%) displayed high cytotoxic effects and were excluded from further experiments. The potential ability of the two CLSs for binding DNA fragments generated by PCR is shown in Figure 2(C). The formation of the CLS–DNA complexes were determined by the intensity decrease of the bands corresponding to free migrating molecules (solid arrows) and by the increase of the bands exhibiting very low or null electrophoretic mobility, which corresponded to nonmigrating molecules complexed to CLS formulations (top of the gels, open arrows).[37] As expected, the two LS formulations did efficiently interact with DNA. In both cases, a complete shift at the top of the gel was obtained when complexes were formed with 25 μg/mL CLSs. On the contrary [left panel of Fig. 2(C)], the neutral LSs did not bind DNA molecules under these experimental conditions. These data demonstrate that both formulations were suitable for the delivery of nucleic acids to target cells without having inhibitory effects on cell growth.

Levitation and movement of LS

In a first set of experiments, we determined the DEP properties of neutral TP-based LSs or LSs containing 6 and 12% DHDAB. As clearly indicated in Figure 3(A–C), three rounds of concentrations were needed to reach the maximum concentration of LSs in the central DEP cage. In the representative experiment shown in Figure 3(A–C), 1.6 V and 100 kHz were applied in 280 m*M* mannitol and 6.25 m*M* KCl.

The quantitative analysis of the representative experiment of Figure 3(A–C) is shown in Figure 3(D) and demonstrated that 43% (open box, one round), 65% (gray box, two rounds), and 75% (black box, three rounds) of neutral LSs were DEP-caged at the central electrode, as programmed, which provided evidence for an efficient DEP-guided migration of neutral LSs. When the same experiment was repeated with LSs containing 6 and 12% DHDAB [Fig. 3(D)], the concentration at the central DEP cage was achieved by 6% DHDAB but not by 12% DHDAB. Therefore, this experiment indicated that increasing the percentage of DHDAB in the preparation of CLSs might interfere with the efficiency of levitation and DEP movement/entrapment in the DEP cages.

Efficiency of the movement and concentration of LSs at different kilohertz values

The experiment depicted in Figure 3 was repeated several times at 100, 300, 500, 700, and 1000 kHz (Fig. 4). The results obtained clearly indicate that neutral LSs could be efficiently concentrated in the center of the SmartSlide under all of the experimental conditions. The best concentrations were obtained at 100 and 300 kHz. LSs containing 6% DHDAB did not concentrate efficiently at 700–1000 kHz. However, efficient DEP caging and concentration were achieved at 100 kHz. By sharp contrast, no efficient

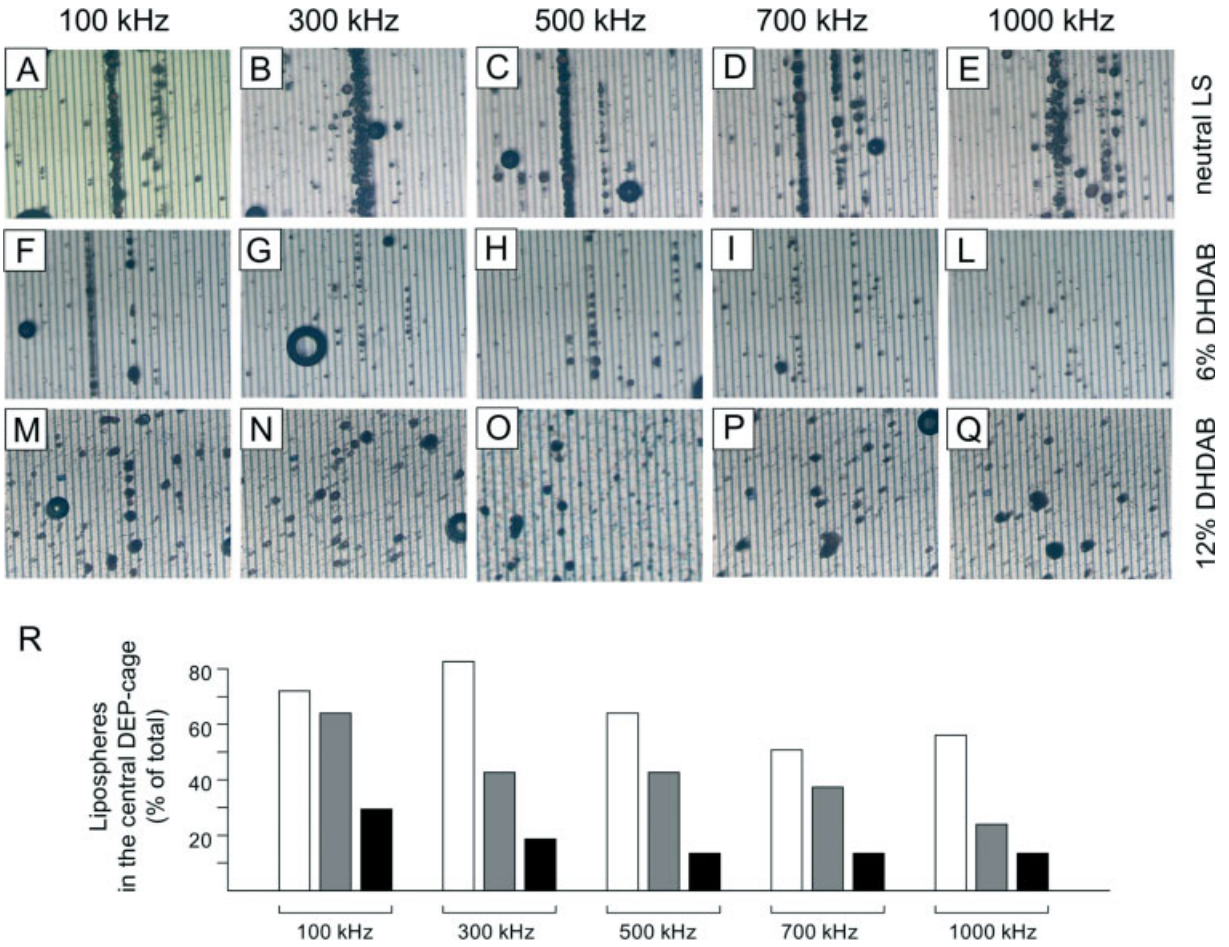

Figure 4 Concentrations of (A–E) neutral LS, (F–L) 6% DHDAB–CLS, and (M–Q) 12% DHDAB–CLS after three rounds at (A,F,M) 100, (B,G,N) 300, (C,H,O) 500, (D,I,P) 700, and (E,L,Q) 1000 kHz. (R) Quantitative analysis of the experimental data shown in panels A–Q. Open histograms represent neutral LS, gray histograms represent 6% DHDAB–CLS, and black histograms represent 12% DHDAB–CLS. Data are expressed as the percentage of LS that were DEP-caged and moved to the SmartSlide central electrode. [Color figure can be viewed in the online issue, which is available at www.interscience.wiley.com.]

concentration was obtained with the 12% DHDAB–LS at any kilohertz value. These data suggested that CLS DEP caging, movement, and concentration depended, within the SmartSlide, on the content of the cationic surfactant. In addition, for the protocol design requiring the DEP caging of LS (e.g., in the case of direct drug delivery), neutral LS can be used at 100–500 kHz; 6% DHDAB–CLS at 100 kHz and 12% DHDAB–CLS are not suitable. For protocols requiring the uncaging of LS, 6% DHDAB–CLS should be used at 300–1000 kHz, whereas 12% DHDAB–CLS can be used at any kilohertz frequency.

DISCUSSION

Microspheres and LS have been largely used in biotechnology to develop approaches useful for diagnosis, gene expression targeting, and drug delivery.[25] Among the different strategies based on microspheres or LSs, several require the coating of these microparticles with monoclonal antibodies recognizing target antigens. An example is magnetic cell sorter technology, which is based on the fact that magnetic activated microspheres exposing monoclonal antibodies might capture target cells; this approach demonstrates that only cells exposing the antigen (and, therefore, bound to the magnetic beads) will be recovered. For instance, Papadimitriou et al.[38] reported immunomagnetic separation with anti-CD34 monoclonal antibodies and paramagnetic microspheres to enrich hematopoietic stem cells from human bone marrow, whole cord blood, or mobilized peripheral blood mononuclear cell collections. Using the magnetic cell sorter, these authors were able to demonstrate that the final product purity was 74.1% CD34+ cells (starting population = 2.3 ± 3.3%) with a 60.3% CD34+ cell yield. In addition to magnetic cell sorting, at the same time,

centrifugation might be carried out with cells and microparticles carrying fluorescence-activated (or radioactivity-labeled) monoclonal antibodies. In this case, fluorescence will be found in the pellet (or cell density fraction) only if the cells are specifically bound to be microparticles. For instance, DeBell et al.[39] developed a centrifugation-based assay to quantify the binding of beads coated with anti-T-cell receptor monoclonal antibodies to T lymphocytes. The mixtures were incubated at 37°C for 10–20 min, and unbound beads were separated from cell-bound beads by Percoll gradient centrifugation. Beads coated with anti-T-cell receptor antibodies formed stable conjugates with cells and were copurified with them.

These approaches require that target cells and functionalized LSs should be coisolated with physical approaches (magnetic precipitation or centrifugation) only when the LSs are exposing molecules specifically recognizing the target cell (antibodies, peptides, aptamers). Cells and microbeads, on the contrary, should not be coisolated when the microparticles are not functionalized or are functionalized with molecules not specific for the target cell.

A second important field based on LSs is cell targeting. In this case, forced interaction between cells and LSs is required. Examples are LS-based cell bombardment, the coprecipitation of cells, LSs with poly(ethylene glycol)-based materials, and the development of bioadhesive LSs.

For instance, microparticle bombardment has been studied by different groups for drug delivery and vaccination.[40–42] Uchida et al.[40] reported data suggesting that the bombardment injection of drug-loaded microspheres by a Helios gun system is a very useful tool for delivering a variety of drugs in powder form to cells.

Vasir et al.[43] reported the use of recent advances in polymer science and drug carrier technologies for the development of novel drug carriers, such as bioadhesive microspheres that have boosted the use of bioadhesion in drug delivery, ranging from small molecules to peptides to macromolecular drugs such as proteins, oligonucleotides, and even DNA. The development of mucus- or cell-specific bioadhesive polymers and the concepts of cytoadhesion and bioinvasion provide unprecedented opportunities for the targeting of drugs to specific cells or intracellular compartments.

In all these cases, forced interactions between LSs and target cells are a requirement for efficient drug delivery.

The use of LSs and DEP-based platforms might be an excellent strategy for the development of protocols mimicking the previously reported technology, including monoclonal-antibody-mediated interactions between LSs and cells as well as forced cell–LS interactions with nonfunctionalized beads. For this reason, it is important to have LS formulations that are able to be entrapped into DEP cages, as well as formulations that do not exhibit this property.

The major result of this study is that neutral LSs or LSs carrying 6% DHDAB can be DEP-caged, levitated, and concentrated to the central cylinder-shaped electrode of a DEP-based lab-on-a-chip platform. Therefore, these LSs appear to be suitable for forced drug delivery when DEP-caged together with target cells.

On the contrary, 12% DHDAB–LS did not exhibit the ability to be DEP-caged and moved throughout the device. Therefore, these LS formulations are suitable for diagnostic protocols aimed at the identification of microparticles within DEP cages only when they are coisolated with target cells in virtue of biomolecular interactions (e.g., following antibody–antigen interactions).

References

1. Medoro, G.; Guerrieri, R.; Manaresi, N.; Nastruzzi, C.; Gambari, R. IEEE Des Test Comput 2007, 24, 26.
2. Altomare, L.; Borgatti, M.; Medoro, G.; Manaresi, N.; Tartagni, M.; Guerrieri, R.; Gambari, R. Biotechnol Bioeng 2003, 82, 474.
3. Gambari, R.; Borgatti, M.; Altomare, L.; Manaresi, N.; Medoro, G.; Romani, A.; Tartagni, M.; Guerrieri, R. Technol Cancer Res Treat 2003, 2, 31.
4. Borgatti, M.; Altomare, L.; Baruffa, M.; Fabbri, E.; Manaresi, N.; Medoro, G.; Romani, A.; Tartagni, M.; Gambari, R.; Guerrieri, R. Int J Mol Med 2005, 15, 913.
5. Borgatti, M.; Altomare, L.; Abonnec, M.; Fabbri, E.; Manaresi, N.; Medoro, G.; Romani, A.; Tartagni, M.; Nastruzzi, C.; Di Croce, S.; Tosi, A.; Mancini, I.; Guerrieri, R.; Gambari, R. Int J Oncol 2005, 27, 1559.
6. Gambari, R.; Borgatti, M.; Fabbri, E.; Gavioli, R.; Fortini, C.; Nastruzzi, C.; Altomare, L.; Abonnec, M.; Manaresi, N.; Medoro, G.; Romani, A.; Tartagni, M.; Guerrieri, R. In Bioarrays, from Basics to Diagnostics; Appasani, K., Ed.; Humana: New York, 2007; p 231.
7. Weigl, B. H.; Hedine, K. Am Clin Lab 2002, 21, 8.
8. Mouradian, S. Curr Opin Chem Biol 2002, 6, 51.
9. Morgan, H.; Hughes; M. P.; Green, N. G. Biophys J 1999, 77, 516.
10. Voldman, J.; Braff, R. A.; Toner, M.; Gray, M. L.; Schmidt, M. A. Biophys J 2001, 80, 531.
11. Gascoyne, P. R.; Vykoukal, J. Electrophoresis 2002, 23, 1973.
12. Pohl, H. A.; Crane, J. S. J Theor Biol 1972, 37, 1.
13. Crane, J. S.; Pohl, H. A. J Theor Biol 1972, 37, 15.
14. Fiedler, S.; Shirley, S. G.; Schnelle, T.; Fuhr, G. Anal Chem 1998, 70, 1909.
15. Huang, Y.; Yang, J.; Wang, X. B.; Becker, F. F.; Gascoyne, P. R. J Hematother Stem Cell Res 1999, 8, 481.
16. Yang, J.; Huang, Y.; Wang, X. B.; Becker, F. F.; Gascoyne, P. R. Biophys J 2000, 78, 2680.
17. Ogata, S.; Yasukawa, T.; Matsue, T. Bioelectrochemistry 2001, 54, 33.
18. Wang, X. B.; Yang, J.; Huang, Y.; Vykoukal, J.; Becker, F. F.; Gascoyne, P. R. Anal Chem 2000, 72, 832.
19. Cortesi, R.; Esposito, E.; Luca, G.; Nastruzzi, C. Biomaterials 2002, 23, 2283.

20. Khopade, A. J.; Shelly, C.; Pandit, N. K.; Banakar, U. V. J Biomater Appl 2000, 14, 389.
21. Bekerman, T.; Golenser, J.; Domb, A. J Pharm Sci 2004, 93, 1264.
22. Barakat, N. S.; Yassin, A. E. Drug Delivery 2006, 13, 95.
23. El-Gibaly, I.; Abdel-Ghaffar, S. K. Int J Pharm 2005, 294, 33.
24. Toongsuwan, S.; Li, L. C.; Erickson, B. K.; Chang, H. C. Int J Pharm 2004, 280, 57.
25. Cortesi, R.; Esposito, E.; Nastruzzi, C. In Lipospheres in Drug Targets and Delivery; Nastruzzi, C., Ed.; CRC: Boca Raton, FL, 2005; p 143.
26. Könnings, S.; Göpferich, A. In Lipospheres in Drug Targets and Delivery; Nastruzzi, C., Ed.; CRC: Boca Raton, FL, 2005; p 67.
27. Schäfer-Korting, M.; Mehnert, W. In Lipospheres in Drug Targets and Delivery; Nastruzzi, C., Ed.; CRC: Boca Raton, FL, 2005; p 127.
28. Domb, A. J.; Ezra, A.; Mizrahi, B. I. In Lipospheres in Drug Targets and Delivery; Nastruzzi, C., Ed.; CRC: Boca Raton, FL, 2005; p 143.
29. Lozzio, C. B.; Lozzio, B. B. Blood 1975, 45, 321.
30. Bianchi, N.; Ongaro, F.; Chiarabelli, C.; Gualandi, L.; Mischiati, C.; Bergamini, P.; Gambari, R. Biochem Pharmacol 2000, 60, 31.
31. Bianchi, N.; Osti, F.; Rutigliano, C.; Corradini, F. G.; Borsetti, E.; Tomassetti, M.; Mischiati, C.; Feriotto, G.; Gambari, R. Br J Haematol 1999, 104, 258.
32. Mischiati, C.; Sereni, A.; Finotti, A.; Breda, L.; Cortesi, R.; Nastruzzi, C.; Romanelli, A.; Saviano, M.; Bianchi, N.; Pedone, C.; Borgatti, M.; Gambari, R. J Biomed Sci 2004, 11, 697.
33. Lampronti, I.; Martello, D.; Bianchi, N.; Borgatti, M.; Lambertini, E.; Piva, R.; Jabbar, S.; Choudhuri, M. S.; Khan, M. T.; Gambari, R. Phytomedicine 2003, 10, 300.
34. Borgatti, M.; Bezzerri, V.; Mancini, I.; Nicolis, E.; Dechecchi, M. C.; Lampronti, I.; Rizzotti, P.; Cabrini, G.; Gambari, R. Biochem Biophys Res Commun 2007, 357, 977.
35. Penolazzi, L.; Zennaro, M.; Lambertini, E.; Tavanti, E.; Torreggiani, E.; Gambari, R.; Piva, R. Mol Pharmacol 2007, 71, 1457.
36. Lambertini, E.; Piva, R.; Khan, M. T.; Lampronti, I.; Bianchi, N.; Borgatti, M.; Gambari, R. Int J Oncol 2004, 24, 419.
37. Mazzitelli, S.; Balestra, C.; Cortesi, R.; Esposito, R.; Nastruzzi, C. Minerva Biotecnol 2007, 19, 33.
38. Papadimitriou, C. A.; Roots, A.; Koenigsmann, M.; Mucke, C.; Oelmann, E.; Oberberg, D.; Reufi, B.; Thiel, E.; Berdel, W. E. J Hematother 1995, 4, 539.
39. DeBell, K. E.; Taplits, M. S.; Hoffman, T.; Bonvini, E. Cell Immunol 1990, 127, 159.
40. Uchida, M.; Natsume, H.; Kobayashi, D.; Sugibayashi, K.; Morimoto, Y. Biol Pharm Bull 2002, 25, 690.
41. Finer, J. J.; Finer, K. R.; Ponappa, T. Curr Top Microbiol Immunol 1999, 240, 59.
42. Praitis, V. Methods Mol Biol 2006, 351, 93.
43. Vasir, J. K.; Tambwekar, K.; Garg, S. Int J Pharm 2003, 255, 13.